

# ADAPTIVE MULTICHANNEL EQUALIZATION APPLIED TO ROOM ACOUSTICS EXPLOITING THE SPARSITY OF TARGET RESPONSE

Rajan S. Rashobh and Andy W. H. Khong

School of Electrical and Electronic Engineering  
Nanyang Technological University, Singapore  
E-mail: raja0042@e.ntu.edu.sg, andykhong@ntu.edu.sg

## ABSTRACT

The adaptive multiple-input/output inverse theorem (A-MINT) multichannel equalization algorithm was proposed to address the computational complexity of the MINT algorithm. However, similar to MINT, A-MINT also assumes an arbitrary modeling delay for the target response which, if inappropriately chosen, results in misconvergence or poor performance. We present a new adaptive algorithm that exploits the sparsity of a target response to estimate equalization filters. The proposed algorithm automatically selects a suitable modeling delay for the equalized response so as to achieve a minimum-norm solution.

**Index Terms**— Adaptive multichannel equalization, dereverberation, acoustic impulse response, sparseness

## 1. INTRODUCTION

Channel equalization techniques have been employed in applications such as speech dereverberation in order to mitigate the effect of multipath propagation. The quality of a speech signal received by a distant microphone within an enclosed environment is often degraded by reverberation [1]. Speech dereverberation algorithms are therefore employed to restore speech quality by suppressing reverberation artifacts. One of the well-known techniques to achieve speech dereverberation is the inverse filtering of received signals using the acoustic impulse responses (AIRs) estimated by blind system identification (BSI) algorithms [2]–[6]. However, since the AIRs are generally non-minimum phase, direct inversion of these AIRs will result in unstable inverse filters.

Single- as well as multi-channel equalization algorithms have been proposed to achieve stable inversion of non-minimum phase AIRs. Multichannel algorithms are, in general, preferred over single-channel algorithms, since the latter result in only approximate equalization [7], [8]. In [8], a multichannel equalization (MCEQ) algorithm based on the multiple-input/output inverse theorem (MINT) has been proposed for achieving exact inverse filters if the channels are co-prime. However, the least-square solution of MINT involves the inversion of a filtering matrix with dimension that

is proportional to the length of AIRs, making it computationally complex for high-order AIRs. To address the computational complexity associated with MINT, the adaptive MINT (A-MINT) algorithm was proposed in [9]. In A-MINT, the inverse filters are iteratively estimated by minimizing a cost function that is formulated from the MINT relation.

MINT and its non-adaptive as well as adaptive variants such as presented in [10]–[15] use a fixed target response with an arbitrarily chosen modeling delay. It has been shown that the equalization performance degrades for an inappropriate choice of modeling delay [10], [16], [17]. In this paper we propose an adaptive MCEQ algorithm that is based on the MINT relation. Unlike A-MINT, the cost function of the proposed algorithm is derived from the sparseness measure of the target response. As opposed to existing algorithms with a fixed target response, the proposed algorithm is able to determine the target response with an appropriate modeling delay during the adaptation process. We note that such an approach, in which the target response is automatically selected by the algorithm, has not been employed for MCEQ in existing literature.

## 2. REVIEW OF MINT AND A-MINT

For an  $M$ -channel acoustic system, and defining  $m$  as the channel index, the MINT algorithm estimates a set of inverse filters  $\mathbf{g}_m = [g_{m,0}, \dots, g_{m,L_g-1}]^T$ ,  $m = 1, \dots, M$ , corresponding to AIR  $\mathbf{h}_m = [h_{m,0}, \dots, h_{m,L_h-1}]^T$  where  $L_g$  and  $L_h$  are the length of  $\mathbf{g}_m$  and  $\mathbf{h}_m$ , respectively. These inverse filters must satisfy the condition [8]

$$\sum_{m=1}^M \mathbf{H}_m \mathbf{g}_m = \mathbf{d}, \quad (1)$$

where  $\mathbf{H}_m$  is a  $L_d \times L_g$  convolution matrix of  $\mathbf{h}_m$ ,  $L_d = L_g + L_h - 1$  and the  $L_d \times 1$  target response

$$\mathbf{d} = [\mathbf{0}_{1 \times \tau}, 1, \mathbf{0}_{1 \times (L_d - \tau - 1)}]^T \quad (2)$$

is a Kronecker delta function while  $\mathbf{0}_{1 \times \tau}$  is a  $1 \times \tau$  null vector. It is important to note that, in practice, a modeling

delay  $\tau$  is introduced to the target response  $\mathbf{d}$  to relax the causality constraint [7], [10]. In addition,  $L_g$  is chosen such that  $L_g \geq L_c$  [18], where the critical length  $L_c = \lceil \frac{L_h-1}{M-1} \rceil$ ,  $M \geq 2$  and  $\lceil \cdot \rceil$  denotes the ceiling operator. The MCEQ filters  $\mathbf{g} = [\mathbf{g}_1^T, \dots, \mathbf{g}_M^T]^T$  can be estimated from (1) in the least-square sense if the channels are co-prime. This estimate can be achieved using

$$\hat{\mathbf{g}} = \arg \min_{\hat{\mathbf{g}}} \|\mathbf{d} - \mathbf{H}\hat{\mathbf{g}}\|_2^2 = \mathbf{H}^+ \mathbf{d}, \quad (3)$$

where  $(\cdot)^+$  is the matrix pseudo-inverse operator,  $\hat{\mathbf{g}}$  is an estimate of  $\mathbf{g}$  and  $\mathbf{H} = [\mathbf{H}_1, \dots, \mathbf{H}_M]$ . In practice,  $\hat{\mathbf{g}}$  is computed using an estimate  $\hat{\mathbf{H}}$  obtained from AIR estimates  $\hat{\mathbf{h}}_m$  via BSI algorithms such as proposed in [2]–[6], i.e.,  $\hat{\mathbf{g}} = \hat{\mathbf{H}}^+ \mathbf{d}$ .

For typical high-order AIRs, the dimension of  $\mathbf{H}$  becomes significantly large. As a consequence, the inversion operation in (3) imposes a high computational load on MINT. In order to avoid direct inversion of  $\mathbf{H}$  and achieve complexity reduction, the A-MINT algorithm has been proposed [9]. The cost function of this least-mean-square based algorithm is derived from (3) and is given by

$$J_{\text{A-MINT}}(n) = \|\mathbf{d} - \mathbf{H}\hat{\mathbf{g}}(n)\|_2^2. \quad (4)$$

The gradient of A-MINT, computed by differentiating (4) w.r.t  $\hat{\mathbf{g}}(n)$ , is given as

$$\nabla J_{\text{A-MINT}}(n) = -2\mathbf{H}^T \mathbf{d} + 2\mathbf{H}^T \mathbf{H}\hat{\mathbf{g}}(n). \quad (5)$$

Defining  $\mu$  as a non-negative step-size, the update equation of A-MINT is expressed as

$$\hat{\mathbf{g}}(n+1) = \hat{\mathbf{g}}(n) - \mu \nabla J_{\text{A-MINT}}(n)|_{\hat{\mathbf{g}}=\hat{\mathbf{g}}(n)}. \quad (6)$$

It has been shown in [10], [16] that an appropriate choice of modeling delay  $\tau$  is essential to achieve good equalization performance. Since it is challenging to find the exact delay in practice, an arbitrary value is often chosen for  $\tau$ . For an inappropriate choice of  $\tau$ , MINT and A-MINT result in an undesired equalization filter solution, giving a distorted output on filtering.

To illustrate the effect of  $\tau$  on the equalization performance of A-MINT, we simulate using a set of  $M = 5$  synthetic AIRs, each of length  $L_h = 1024$ , generated using the method of images [19]. We have used a sampling frequency  $f_s = 16$  kHz with reverberation time  $T_{60} = L_h/f_s$ . Equalization was then achieved using A-MINT with  $L_g = L_c$  and  $\mu = 0.5$ , for  $\tau = 0, L_h/4, L_h/2$ , and  $3L_h/4$ . To quantify the equalization performance, we employed

$$\eta(n) = 10 \log_{10}[1 - \gamma(n)] \text{ dB}, \quad (7)$$

where  $\gamma(n)$  is the spectral flatness measure (SFM) [20] of the estimated response  $\hat{\mathbf{d}}(n) = \mathbf{H}\hat{\mathbf{g}}(n)$ . The SFM is defined as the ratio of the geometric mean of a spectrum to its arithmetic

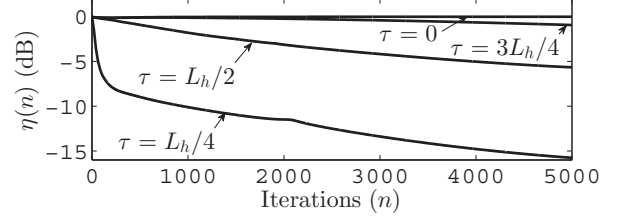


**Fig. 1.** Variation of  $\eta$  as a function of  $\tau$ , for A-MINT.

mean and hence, if  $\hat{\mathbf{d}}(n)$  is a Dirac function having a flat magnitude spectrum,  $\eta(n) = -\infty$  dB giving perfect equalization.

The variation of  $\eta(n)$  for each  $\tau$  is plotted in Fig. 1 and we note that, among the given  $\tau$  values,  $\tau = L_h/4$  achieves the best equalization performance for the given set of AIRs. On the other hand, for  $\tau = 0$ , A-MINT does not converge and this results in an undesired response. These results show that the performance of A-MINT is highly dependent on  $\tau$  and hence it is important to select an appropriate value of  $\tau$ .

### 3. THE PROPOSED AMCEQ-SP ALGORITHM

The sparseness of an arbitrary  $L \times 1$  vector  $\mathbf{v}$  can be quantified by computing the sparseness measure [21], [22]

$$\xi(\mathbf{v}) = \frac{\sqrt{L} - (\|\mathbf{v}\|_1 / \|\mathbf{v}\|_2)}{\sqrt{L} - 1}, \quad (8)$$

where  $0 \leq \xi(\mathbf{v}) \leq 1$ . While  $\xi(\mathbf{v}) = 1$  for a perfectly sparse vector with only a single non-zero element, a fully dispersive vector with elements having the same magnitude results in  $\xi(\mathbf{v}) = 0$ .

From (2) we note that, the target response  $\mathbf{d}$  is a perfectly sparse vector corresponding to  $\xi(\mathbf{d}) = 1$ . We therefore exploit the sparseness measure of  $\hat{\mathbf{d}}(n)$  for estimating MCEQ filters. The proposed adaptive MCEQ with sparseness constraint (AMCEQ-SP) algorithm is derived from the minimization criteria given by

$$\hat{\mathbf{g}}(n) = \arg \min_{\hat{\mathbf{g}}(n)} \{1 - \xi[\mathbf{H}\hat{\mathbf{g}}(n)]\}^2. \quad (9)$$

From (9), a cost function is constructed as

$$J(n) = \left[1 - \frac{\sqrt{L_d} - (\|\mathbf{H}\hat{\mathbf{g}}(n)\|_1 / \|\mathbf{H}\hat{\mathbf{g}}(n)\|_2)}{\sqrt{L_d} - 1}\right]^2. \quad (10)$$

It is important to note that minimization of (10) implies  $\|\mathbf{H}\hat{\mathbf{g}}(n)\|_1 = \|\mathbf{H}\hat{\mathbf{g}}(n)\|_2$ . The gradient of this iterative algorithm is subsequently obtained by differentiating (10) w.r.t  $\hat{\mathbf{g}}(n)$  as

$$\begin{aligned} \nabla J_f(n) &= \frac{\partial J(n)}{\partial \hat{\mathbf{g}}(n)} \\ &= \frac{2\{1 - \xi[\mathbf{H}\hat{\mathbf{g}}(n)]\}}{\sqrt{L_d} - 1} \left\{ \frac{\mathbf{H}^T \text{sgn}[\mathbf{H}\hat{\mathbf{g}}(n)]}{\|\mathbf{H}\hat{\mathbf{g}}(n)\|_2} - \frac{\|\mathbf{H}\hat{\mathbf{g}}(n)\|_1 \mathbf{H}^T [\mathbf{H}\hat{\mathbf{g}}(n)]}{2\|\mathbf{H}\hat{\mathbf{g}}(n)\|_2^2} \right\}, \end{aligned} \quad (11)$$

where  $\text{sgn}(\cdot)$  is an element-wise sign function defined as

$$\text{sgn}(v) = \begin{cases} v/|v| & v \neq 0, \\ 0 & v = 0. \end{cases}$$

Applying the gradient obtained in (11) we achieve the update equation of the proposed AMCEQ-SP algorithm as

$$\hat{\mathbf{g}}'(n+1) = \hat{\mathbf{g}}(n) - \frac{\mu}{\|\mathbf{h}\|_2^2} \nabla J_f(n), \quad (12)$$

$$\hat{\mathbf{g}}(n+1) = \text{sgn}[d'(n+1, \tau+1)] \frac{\hat{\mathbf{g}}'(n+1)}{\|\hat{\mathbf{d}}'(n+1)\|_2} \quad (13)$$

where  $\hat{\mathbf{d}}'(n+1) = \mathbf{H}\hat{\mathbf{g}}'(n+1)$ ,  $\mathbf{h} = [\mathbf{h}_1^T, \dots, \mathbf{h}_m^T]^T$  and  $d'(n, \tau+1)$  is the largest-magnitude coefficient in  $\hat{\mathbf{d}}'(n)$ . In (12) we have normalized  $\mu$  in order to minimize its sensitivity to variations in the energy of  $\mathbf{h}$ .

In (13) we have employed normalization in order to impose a unit-norm constraint on  $\hat{\mathbf{d}}(n+1)$ , i.e.,  $\|\mathbf{H}\hat{\mathbf{g}}(n+1)\|_2 = 1$ . This unit-norm constraint in turn simplifies the gradient as

$$\nabla J_f(n) = \frac{2\{1-\xi[\mathbf{H}\hat{\mathbf{g}}(n)]\}}{\sqrt{L_d-1}} \{\mathbf{H}^T \text{sgn}[\mathbf{H}\hat{\mathbf{g}}(n)] - 0.5\|\mathbf{H}\hat{\mathbf{g}}(n)\|_1 \mathbf{H}^T [\mathbf{H}\hat{\mathbf{g}}(n)]\} \quad (14)$$

after the first iteration. The gradient given by (11) enforces only sparseness without taking the magnitude of the largest nonzero coefficient of equalized response into account. Hence, in order to achieve a response with a non-negative largest peak we apply a magnitude correction in (13) by multiplying with  $\text{sgn}[d'(n+1, \tau+1)]$ . Since initialization using a null vector will result in numerical errors in (11) we use, in this work,  $\hat{\mathbf{g}}_m(0) = [\delta, \mathbf{0}_{1 \times L_g-1}]^T$ , where  $\delta = 10^{-3}$ .

It is also important to note that the gradient of AMCEQ-SP given in (11) is derived so as to enforce sparsity in  $\hat{\mathbf{d}}(n)$ . As a result,  $\hat{\mathbf{g}}$  is estimated such that all but one coefficient in  $\hat{\mathbf{d}}(n)$  are attracted towards zero magnitude at each iteration. Since no constraint has been imposed on  $\tau$ , the algorithm converges to a minimum-norm solution having an appropriate  $\tau$ .

We now analyze the convergence behavior of the proposed AMCEQ-SP algorithm using the general update equation given in (12). In this analysis, for simplicity and mathematical tractability, we do not consider the energy constraint and magnitude correction which are applied in (13) for scaling  $\hat{\mathbf{d}}'(n)$ . Defining  $\Delta\hat{\mathbf{g}}'(n+1) = \hat{\mathbf{g}}'(n+1) - \mathbf{g}'$ , where  $\mathbf{g}'$  is the true solution of (12), we can write, using (12),

$$\begin{aligned} \Delta\hat{\mathbf{g}}'(n+1) &= \Delta\hat{\mathbf{g}}'(n) - \mu' \nabla J_f(n) \\ &= \Delta\hat{\mathbf{g}}'(n) + \mu' \rho(n) \left\{ \frac{\mathbf{H}^T \text{sgn}[\hat{\mathbf{d}}'(n)]}{\|\hat{\mathbf{d}}'(n)\|_2} - \frac{\mathbf{H}^T \mathbf{H}\hat{\mathbf{g}}'(n) \|\hat{\mathbf{d}}'(n)\|_1}{2\|\hat{\mathbf{d}}'(n)\|_2^3} \right\}, \end{aligned} \quad (15)$$

where  $\rho(n) = 2\{\xi[\hat{\mathbf{d}}'(n)] - 1\}/(\sqrt{L_d} - 1)$  and  $\mu' = \frac{\mu}{\|\mathbf{h}\|_2^2}$ . Defining  $\rho'(n) = \rho(n)\|\hat{\mathbf{d}}'(n)\|_1/2\|\hat{\mathbf{d}}'(n)\|_2^3$  and taking the

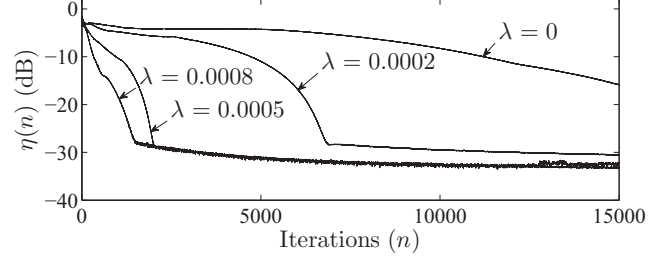


Fig. 2. Variation of  $\eta$  as a function of  $\lambda$ , for AMCEQ-SP.

expectation on both sides of (15) we obtain

$$\begin{aligned} E[\Delta\hat{\mathbf{g}}'(n+1)] &= \left[ \mathbf{I}_{L_d \times L_d} - \mu' \mathbf{R} \right] E[\Delta\hat{\mathbf{g}}'(n)] - \\ &\quad \mu' \mathbf{H}^T E \left[ \frac{\rho(n) \text{sgn}[\hat{\mathbf{d}}'(n)]}{\|\hat{\mathbf{d}}'(n)\|_2} + \rho'(n) \mathbf{d}' \right], \end{aligned} \quad (16)$$

where  $\mathbf{I}_{L_d \times L_d}$  is the  $L_d \times L_d$  identity matrix,  $\mathbf{d}' = \mathbf{H}\mathbf{g}'$  and  $\mathbf{R} = E[\rho'(n)]\mathbf{H}^T\mathbf{H}$ . We note that, since  $E[\hat{\mathbf{g}}'(n)] = E[\Delta\hat{\mathbf{g}}'(n)] + \mathbf{g}'$ , AMCEQ-SP can converge in the limit given by

$$E[\hat{\mathbf{g}}'(\infty)] = - \frac{\mathbf{H}^+ E\{\text{sgn}[\hat{\mathbf{d}}'(\infty)]\}}{E \left[ \frac{\|\hat{\mathbf{d}}'(\infty)\|_1}{2\|\hat{\mathbf{d}}'(\infty)\|_2^3} \right] E[\|\hat{\mathbf{d}}'(\infty)\|_2]}. \quad (17)$$

### 3.1. $L_1$ -norm constraint for faster convergence

For AMCEQ-SP with the unit-norm constraint, since  $\|\hat{\mathbf{d}}(n)\|_2 = 1$ , in order to achieve  $\xi[\hat{\mathbf{d}}(n)] = 1$  it is required that  $\|\hat{\mathbf{d}}(n)\|_1 = 1$ . Therefore, to improve the convergence rate of the energy constrained AMCEQ-SP, we introduce a penalty function defined as

$$J_p = 1 - \|\mathbf{d}(n)\|_1 \quad (18)$$

to the cost function. This penalty function is derived so as to constrain the  $L_1$ -norm of  $\hat{\mathbf{d}}(n)$  to unity. The penalty term derived from (18) is given by

$$\nabla J_p(n) = -2(1 - \|\mathbf{d}(n)\|_1) \mathbf{H}^T \text{sgn}[\hat{\mathbf{d}}(n)]. \quad (19)$$

The modified gradient of the proposed AMCEQ-SP algorithm incorporating the penalty function is therefore given as

$$\nabla J(n) = \nabla J_f(n) + \lambda \nabla J_p(n), \quad (20)$$

where  $\lambda$  is a weighting factor. Since obtaining a closed-form solution is challenging, in this work, we choose an arbitrary value for  $\lambda$ .

## 4. SIMULATION RESULTS

We first examine the effect of  $\lambda$  on the convergence performance of AMCEQ-SP using five synthetic AIRs, each of length  $L_h = 2048$ , generated using the same simulation

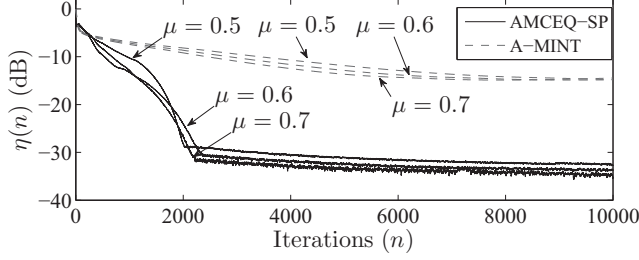


Fig. 3. Variation of  $\eta$  as a function of  $\mu$ .

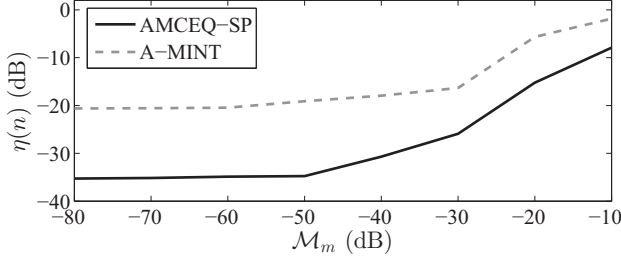


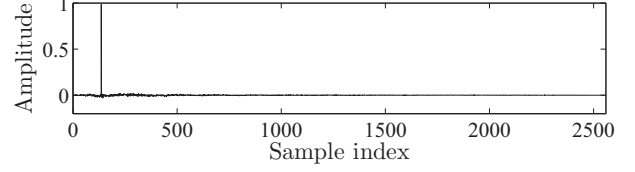
Fig. 4. Equalization performance of AMCEQ-SP and A-MINT in the presence of system mismatch  $\mathcal{M}_m$ .

setup described in Section 2, and  $\mu = 0.5$ . From the convergence performance curves shown in Fig. 2 we note that when  $\lambda = 0$ , i.e., the  $L_1$  norm penalty function is not applied, the algorithm converges at a slow rate. With the application of the penalty function, rate of convergence increases with  $\lambda$ .

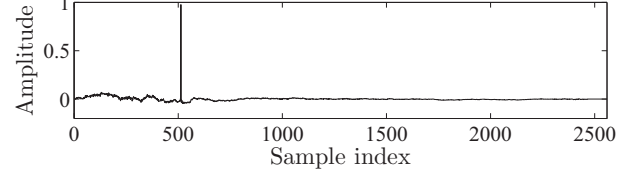
The convergence performance of the proposed AMCEQ-SP algorithm and A-MINT is next illustrated for various  $\mu$  using the same simulation setup. In this simulation, we have selected, for A-MINT,  $\tau = L_h/4$  (which gave the best performance as shown in Fig. 1.) With  $L_g = L_c$  and  $\lambda = 5 \times 10^{-4}$  for AMCEQ-SP,  $\eta(n)$  was computed for different step-sizes and illustrated in Fig. 3. We note from this result that unlike A-MINT with performance being limited by the choice of  $\tau$  AMCEQ-SP achieves good convergence performance with  $\eta < 30$  dB.

Equalization performance in the presence of channel estimation error is also illustrated using five recorded AIRs obtained from the MARDY database [23]. The AIRs were first downsampled to 16 kHz and subsequently truncated to  $L_h = 2048$ . AIR estimation is simulated by perturbing the AIRs using  $\hat{\mathbf{h}}_m = (\mathbf{I}_{L_h \times L_h} + \mathcal{E}_m)\mathbf{h}_m$ , where  $\mathcal{E}_m = \text{diag}\{\epsilon_{m,0}, \dots, \epsilon_{m,L_h-1}\}$ ,  $m = 1, \dots, M$ , and  $\epsilon_{m,i}$  is a zero-mean white Gaussian random sequence. Equalization of  $\mathbf{h}_m$  was then achieved with the inverse filters estimated using  $\hat{\mathbf{h}}_m$  for different system mismatch  $\mathcal{M}_m = 10 \log_{10} \sigma_\epsilon^2$  dB, where  $\sigma_\epsilon^2$  is the variance of  $\epsilon_{m,i}$ ,  $i = 0, \dots, L_h - 1$ .

We illustrate, in Fig. 4, the variation of  $\eta$  with  $\mathcal{M}_m$  at  $n = 1 \times 10^4$ th iteration for AMCEQ-SP with  $\lambda = 5 \times 10^{-4}$  and A-MINT with  $\tau = L_h/4$ . We have used  $\mu = 0.5$  for both algorithms. These results show that, for both algorithms, the equalization performance degrades with increasing sys-



(a)



(b)

Fig. 5. Equalized response obtained for (a) AMCEQ-SP, and (b) A-MINT.

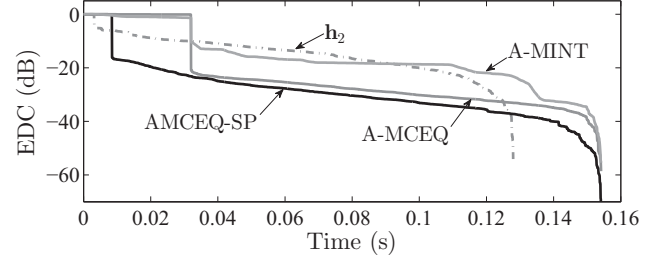


Fig. 6. EDC obtained for  $\mathcal{M}_m = -20$  dB.

tem mismatch. Compared to A-MINT with an arbitrarily selected  $\tau = L_h/4$ , AMCEQ-SP achieves better equalization performance. The equalized responses estimated with both algorithms for  $\mathcal{M}_m = -20$  dB are shown in Fig. 5. We note that AMCEQ-SP with  $\eta = -15.6$  dB achieves a  $\hat{\mathbf{d}}$  that is closer to a Dirac function compared to A-MINT which achieves  $\eta = -5.4$  dB only.

To further illustrate the performance improvement obtained with AMCEQ-SP the energy decay curves (EDCs) [24] obtained for  $\mathbf{h}_2$ , AMCEQ-SP, A-MINT and recently proposed A-MCEQ [15] are depicted in Fig. 6. In this plot, good equalization is exhibited by a low EDC value. Comparing the EDCs it can be seen that AMCEQ-SP achieves better reverberation suppression than A-MINT and A-MCEQ.

## 5. CONCLUSION

We proposed a new adaptive MCEQ algorithm. As opposed to existing MINT-based algorithms which model the desired response with an arbitrary delay the proposed AMCEQ-SP algorithm converges to a solution with an appropriate delay for the equalized response. Simulation results show that AMCEQ-SP can achieve good equalization performance even in the presence of AIR estimation error. The proposed  $L_1$ -norm constraint helps the algorithm to achieve fast convergence.

## 6. REFERENCES

- [1] P. A. Naylor and N. D. Gaubitch, "Speech dereverberation," in *Proc. Int. Workshop Acoust. Echo Noise Control*, Sep. 2005.
- [2] E. Moulines, P. Duhamel, J. Cardoso, and S. Mayrargue, "Subspace methods for the blind identification of multichannel FIR filters," in *Proc. IEEE Int. Conf. Acoust., Speech, and Signal Process.*, Feb. 1995, pp. 516–525.
- [3] Y. Hua, "Fast maximum likelihood for blind identification of multiple fir channels," *IEEE Trans. Signal Process.*, vol. 86, pp. 1951–1968, Oct 1996.
- [4] Y. Huang and J. Benesty, "Adaptive multi-channel least mean square and Newton algorithms for blind channel identification," *Signal Process.*, vol. 82, pp. 1127–1138, Aug. 2002.
- [5] Y. Huang and J. Benesty, "A class of frequency-domain adaptive approaches to blind multichannel identification," *IEEE Trans. Signal Process.*, vol. 51, no. 1, pp. 11–24, Jan. 2003.
- [6] S. Gannot and M. Moonen, "Subspace methods for multimicrophone speech dereverberation," *EURASIP J. Applied Signal Process.*, vol. 11, pp. 1074–1090, 2003.
- [7] J. Mourjopoulos, P. Clarkson, and J. Hammond, "A comparative study of least-squares and homomorphic techniques for the inversion of mixed phase signals," in *Proc. IEEE Int. Conf. Acoust., Speech, and Signal Process.*, May 1982, vol. 7, pp. 1858–1861.
- [8] M. Miyoshi and Y. Kaneda, "Inverse filtering of room acoustics," *IEEE Trans. Acoust., Speech and Signal Process.*, vol. 36, no. 2, pp. 145–152, Feb. 1988.
- [9] W. Zhang, A. W. H. Khong, and P. A. Naylor, "Adaptive inverse filtering of room acoustics," in *Proc. IEEE Asilomar Conf. on Signals, Systems and Computers*, 2008, pp. 788–792.
- [10] T. Hikichi, M. Delcroix, and M. Miyoshi, "Inverse filtering for speech dereverberation less sensitive to noise and room transfer function fluctuations," *EURASIP J. Advances in Signal Process.*, vol. 2007:34013, no. 1, pp. 1–12, 2007.
- [11] L. Liao and A. W. H. Khong, "Adaptive channel equalization of room acoustics exploiting sparseness constraint," *IEEE Signal Process. Lett.*, vol. 18, no. 4, pp. 275–278, Apr. 2011.
- [12] R. S. Rashobh, D. Liu, and A. W. H. Khong, "An adaptive subspace based multichannel equalization algorithm for room acoustics equalization with sparseness constraint," in *Proc. IEEE Int. Conf. Info. Comm. Signal Process.*, Dec. 2011, pp. 1–5.
- [13] I. Kodrasi and S. Doclo, "Robust partial multichannel equalization techniques for speech dereverberation," in *Proc. IEEE Int. Conf. Acoust., Speech, and Signal Process.*, Mar. 2012, pp. 21–24.
- [14] F. Lim and P. A. Naylor, "Relaxed multichannel least squares with constrained initial taps for multichannel dereverberation," in *Proc. Int. Workshop Acoust. Echo Noise Control*, Sep. 2012.
- [15] R. S. Rashobh and A. W. H. Khong, "A variable step-size multichannel equalization algorithm exploiting sparseness measure for room acoustics," in *Proc. IEEE Int. Symp. Circuits and Systems*, May. 2012, pp. 2753–2756.
- [16] T. Hikichi, M. Delcroix, and M. Miyoshi, "Inverse filtering for speech dereverberation less sensitive to noise," in *Proc. Int. Workshop Acoust. Echo Noise Control*, Sep. 2006, pp. 1–4.
- [17] T. Hikichi, M. Delcroix, and M. Moiyoshi, "On robust inverse filter design for room transfer function fluctuations," in *Proc. European Signal Process. Conf.*, Sep. 2006.
- [18] G. Harikumar and Y. Bresler, "FIR perfect signal reconstruction from multiple convolutions: minimum deconvolver orders," *IEEE Trans. Signal Process.*, vol. 46, no. 1, pp. 215–218, 1998.
- [19] J. B. Allen and D. A. Berkley, "Image method for efficiently simulating small room acoustics," *J. Acoust. Soc. Amer.*, vol. 65, no. 4, pp. 943–950, Apr. 1979.
- [20] J. D. Johnston, "Transform coding of audio signals using perceptual noise criteria," *IEEE J. Select. Areas Commun.*, vol. 6, no. 2, pp. 314–323, Feb. 1988.
- [21] P. O. Hoyer, "Non-negative matrix factorization with sparseness constraints," *J. Machine Learning Res.*, vol. 5, pp. 1457–1469, Nov. 2004.
- [22] P. Loganathan, A. W. H. Khong, and P. A. Naylor, "A class of sparseness-controlled algorithms for echo cancellation," *IEEE Trans. Audio, Speech, and Lang. Process.*, vol. 17, no. 8, pp. 1591–1601, 2009.
- [23] J. Y. C. Wen, N. D. Gaubitch, E. A. P. Habets, T. Myatt, and P. A. Naylor, "Evaluation of speech dereverberation algorithms using the MARDY database," in *Proc. Int. Workshop Acoust. Echo Noise Control*, Sep. 2006.
- [24] P. A. Naylor and N. D. Gaubitch, *Speech Dereverberation*, Springer Publishing Company Inc., 1st edition, 2010.